

Hydrothermal depolymerization of biorefinery lignin-rich streams: Influence of reaction conditions and catalytic additives on the organic monomers yields in biocrude and aqueous

Original

Hydrothermal depolymerization of biorefinery lignin-rich streams: Influence of reaction conditions and catalytic additives on the organic monomers yields in biocrude and aqueous phase / Dell'Orco, S.; Miliotti, E.; Lotti, G.; Rizzo, A. M.; Rosi, L.; Chiaramonti, D.. - In: ENERGIES. - ISSN 1996-1073. - 13:5(2020). [10.3390/en13051241]

Availability:

This version is available at: 11583/2995519 since: 2024-12-17T12:30:06Z

Publisher:

MDPI AG

Published

DOI:10.3390/en13051241

Terms of use:

This article is made available under terms and conditions as specified in the corresponding bibliographic description in the repository

Publisher copyright

(Article begins on next page)

Article

Hydrothermal Depolymerization of Biorefinery Lignin-Rich Streams: Influence of Reaction Conditions and Catalytic Additives on the Organic Monomers Yields in Biocrude and Aqueous Phase

Stefano Dell’Orco ^{1,2}, Edoardo Miliotti ¹, Giulia Lotti ¹, Andrea Maria Rizzo ¹, Luca Rosi ^{1,3} and David Chiaramonti ^{1,4,*}

¹ RE-CORD, Viale Kennedy 182, Scarperia e San Piero, 50038 Florence, Italy; stefano.dellorco@unifi.it (S.D.O.); edoardo.miliotti@re-cord.org (E.M.); giulia.lotti@re-cord.org (G.L.); andreamaria.rizzo@re-cord.org (A.M.R.); luca.rosi@re-cord.org (L.R.)

² Department of Industrial Engineering, University of Florence, Viale Morgagni 40, 50135 Florence, Italy

³ Chemistry Department “Ugo Schiff”, University of Florence, Via della Lastruccia, Sesto Fiorentino, 3-13 50019 Florence, Italy

⁴ “Galileo Ferraris” Energy Department, Polytechnic of Turin, Corso Duca degli Abruzzi 24, I-10129 Torino, Italy

* Correspondence: david.chiaramonti@polito.it

Received: 27 January 2020; Accepted: 3 March 2020; Published: 7 March 2020



Abstract: Hydrothermal depolymerization of lignin-rich streams (LRS) from lignocellulosic ethanol was successfully carried out in a lab-scale batch reactors unit. A partial depolymerization into oligomers and monomers was achieved using subcritical water as reaction medium. The influence of temperature (300–350–370 °C) and time (5–10 minutes) was investigated to identify the optimal condition on the monomers yields in the lighter biocrude (BC1) and aqueous phase (AP) fractions, focusing on specific phenolic classes as well as carboxylic acids and alcohols. The effect of base catalyzed reactions (2–4 wt. % of KOH) was compared to the control tests as well as to acid-catalyzed reactions obtained with a biphasic medium of supercritical carbon dioxide (sCO₂) and subcritical water. KOH addition resulted in enhanced overall depolymerization without showing a strong influence on the phenolic generation, whereas sCO₂ demonstrated higher phenolic selectivity even though no effect was observed on the overall products mass yields. In conclusion, a comparison between two different biocrude collection procedures was carried out in order to understand how the selected chemical extraction mode influences the distribution of compounds between BC1 and AP.

Keywords: Biorefinery; hydrothermal liquefaction; lignin stream recovery; lignin depolymerization; catalyzed liquefaction; supercritical carbon dioxide; biocrude and aqueous phase characterization; liquefaction conditions; biocrude solvent extraction

1. Introduction

Lignin is one of the main constituents of lignocellulosic biomass, and making up to 15–35 wt. % of the total organic matter weight, carrying also the highest specific energy content compared to cellulose and hemicellulose [1–3]. The global amount of lignin estimated in the Earth’s surface is 300 billion tons and annually increases by around 20 billion tons [4]. Lignin separation from cellulose and hemicellulose takes place extensively in the second generation lignocellulosic ethanol biorefineries and pulp and papers industry [5]. In order to estimate the potential of lignin from lignocellulosic ethanol biorefinery, an European study from E4 Tech [6] investigated scenarios for the growth of

biorefinery industry under a favorable supporting policy as the one foreseen by the Directive (EU) 2018/2001 of the European Parliament and of the Council of 11 December 2018 on the promotion of the use of energy from renewable sources (in short Renewable Energy Directive - RED II). Future scenario foresees a ramp up in Europe from one plant producing at commercial scale in 2017 to 46 plants in 2030. From 2022 to 2025, 3–4 new plants per year across Europe are expected, but from 2025 to 2030, this rate should increase to an average of 6–7 new plants commencing production annually. Consequently, the amount of lignin co-product will considerably increase, rising the interests on its conversion pathways to chemicals or fuels precursors, reducing CO₂ emissions and the need for fossil resources. For these reasons, the economic viability of future biorefineries will mostly depend on efficient conversion of each biomass constituent, transforming both cellulose/hemicellulose and lignin into value-added compounds.

For decades the pulp industry has been converting lignocellulosic materials into valuable fibers and products [7]. Second-generation biomass conversion technologies are nowadays able to produce renewable chemicals and biofuels only from the cellulose and hemicellulose fraction at commercial scale. However, due to its aromatic structure, lignin has unique properties that makes this material a highly interesting biopolymer for further processing [8]. Lignin-rich streams (LRS) from lignocellulosic ethanol contain high amount of water (60–70 wt. %) [9] making the material suitable for hydrothermal liquefaction (HTL) as first-step for product valorization. Among other thermochemical conversion strategies, HTL is a process recommended for wet biomass: the reactions are generally carried out in water at 280–370 °C and between 10 and 25 MPa. At these conditions, the water is in its subcritical state and the dielectric constant of water decreases; thus, behaving like a non-polar organic solvent breaking structural links of the biomass matrix. In these physical conditions it also has enhanced acidity donating protons to molecules, impacting the decomposition process [10]. The main HTL reaction products are biocrude, char, water-soluble substances, and gas (mostly CO₂). Efforts have already been made to convert lignin feedstocks into valuable products through liquefaction. Lignin from paper and pulp industries (Kraft lignin) have been depolymerized by Yuan et al. [11] at 220–300 °C in a water-ethanol medium with NaOH as catalyst and phenol as capping agent, observing a decrement in the products molecular weight distribution, optimized at 260 °C and 3 h of residence time. On the other hand, Nguyen et al. [12] studied the effect of higher temperature (290–370 °C) on Kraft lignin liquefaction in subcritical water using ZrO₂/K₂CO₃ as catalysts and phenol as the co-solvent, characterizing the composition of the aqueous phase and the biocrude at different temperature levels and catalyst load. Regarding lignin from lignocellulosic ethanol, the conversion into valuable products through HTL has been investigated by other authors in the past. Jensen et al. [13] investigated the conversion of enzymatic hydrolysis lignin, focusing in how plant species and pretreatment severity affect the HTL product composition and lignin depolymerization. Katahira et al. [14] investigated base catalyzed lignin depolymerization from five different feedstocks, evaluating product composition after 40 min of reaction time, varying reaction temperature (270–300–330 °C) and amount of alkaline additive. Nielsen et al. [15], studied batch liquefaction of lignin from enzymatic hydrolysis in supercritical ethanol by varying reaction temperature (250–450 °C), reaction time (0–8 h), and solvent:lignin ratio (0–40 g in 100 mL), in absence of catalysts.

In addition, the effect of KOH was evaluated, highlighting how the liquefaction conversion is influenced. A variation of initial pH, with the addition of KOH, have already been demonstrated as an effective method to optimize the depolymerization of Kraft lignin by Belkheiri et al. [16]. In this study, its effect has been evaluated on a different type of lignin that was found to generate a higher acidity in the aqueous product, thus finding always a low pH in the residual aqueous phase regardless of the initial amount of KOH. On the other hand, the effect of an acid reaction environment has been tested with the use of supercritical CO₂ (sCO₂). Indeed, concentrated carbon dioxide is always produced in large amount during sugars fermentation: theoretically, 1 mol of glucose yields 2 mol of ethanol and 2 mol of CO₂, and the worldwide carbon dioxide emission due to first and second generation ethanol fermentation plants was estimated to be 49.8 Mt [17,18]. Some efforts have been made to capture and

store CO₂ in order to further reduce the carbon footprint of the technology through bio-energy with carbon capture and storage (BECCS) technologies as, differently to fossil fuels, the CO₂ produced in ethanol plants came from renewable sources and its capture would determine a net atmospheric carbon removal [17,19]. Furthermore, the use of CO₂ at its supercritical state has been extensively investigated as selective solvent for phenolic compounds separation and extraction [20–23]. Moreover, Numan-Al-Mobin [24] converted alkali lignin using a mixture of subcritical water and supercritical carbon dioxide, varying temperature (250, 300, and 350 °C) and water-to-sCO₂ ratio (1:5, 1:2, 1:1, and 2:1) showing an enhanced yield of specific phenolic compounds and suggesting a conversion mechanism driven by the heterogeneous acid catalytic activity of the dissolved CO₂. In another study, Chan et al. [25] studied the effect of supercritical carbon dioxide on the liquefaction of palm kernel shell, suggesting an improved biocrude yield at lower temperature due to the higher CO₂ dissolution in water enhancing the protons availability in the water medium. In the present work, the measured products yield and the selectivity towards phenolic species have been evaluated at 300 °C, comparing the results to the ones observed in uncatalyzed and base catalyzed reactions.

In a perspective of industrial applications, HTL should ideally target high yield, minimization of reaction time and the increasing in solid load of the processed slurry. For these reasons, in a previously published manuscript [26], the authors suggested how the HTL conditions can be tuned to optimize the process in term of biocrude mass yield testing in a batch-reactor unit, short residence time (5–10 min) and two level of solid load (10–20 wt. % of dry biomass to water ratio, B/W). In addition, the B/W ratio influence to the process was found to be not statistically significant in regards to the light biocrude mass yield and in this work, it was chosen to analyze the results from experiments with 10 wt. % B/W. These previous results suggested different ways for process optimization, affecting the characteristics and the amount of produced biocrude. Thus, to further improve the understanding of HTL-based conversion of lignin-rich stream, the present work intends to add specific know-how on the influence of several reaction conditions in subcritical water such as temperature, residence time, base or acid catalyzed reactions, focusing on the monomeric composition of the liquid products. A critical characterization of the HTL products is here presented, showing how valuable monomers from the LRS conversion can be optimized in terms of yield and how the reaction conditions affect the depolymerization process and products.

2. Materials and Methods

2.1. Feedstock Characterization

Lignin-rich material was obtained from an industrial demo-scale lignocellulosic ethanol plant after ethanol distillation and water mechanical separation. The original biomass feedstock used in the ethanol biorefinery was hardwood, specifically poplar. Carbon, hydrogen, nitrogen, and sulfur (CHN-S) content was quantified using a Leco (St. Joseph, MI, USA) TruSpec (UNI EN 15104, ASTM D4239) and oxygen was obtained by difference. LRS moisture, ash content and volatile matter were determined in a Leco TGA 701 (UNI EN 13040, UNI EN 14775, UNI EN 15148) and fixed carbon was calculated by difference. The feedstock was further characterized after mixing solid particles of lignin with water for the slurry preparation, quantifying the water-soluble compounds in a LC-20 AT Prominence (Shimadzu, Kyoto, Japan) prior to the hydrothermal reactions. The HPLC apparatus is equipped with a refractive index detector, a Hi-Plex H column 300 × 7.7 mm and a guard column PL Hi-Plex H 50 × 7.7 mm (Agilent, Santa Clara, CA, USA), operating at 55 °C with a flow of 0.6 mL min⁻¹ with 0.005 M sulfuric acid as mobile phase. Moreover the percentage of lignin and structural sugars were determined accordingly to the NREL/TP-510-42618 procedure [27].

2.2. Microreactors Test Bench for Screening Reaction Conditions

Biocrude and aqueous phase samples from hydrothermal liquefaction were obtained in a custom-made Micro-Reactor Test Bench (MRTB) described in previous publications [26,28]. In

brief, prior to experiments a slurry sample was prepared stirring dried feedstock in ultrapure water ($0.055 \mu\text{S cm}^{-1}$) at the desired biomass-to-water mass ratio. For each test, 33 g of slurry were inserted into a 43 mL stainless steel reactor. A leakage test was performed with argon pressurized at 8 MPa before purging the system with nitrogen (0.5 MPa). An initial pressure of 3 MPa was set using argon and the reactor was afterwards immersed into a fluidized sand bath previously heated at the requested temperature. Evaluation of residence time started when the temperature in the reactor reached 2°C below the set temperature, the reactor was then rapidly cooled by immersion into a water bath.

Two biocrude fractions were always recovered at the end of each test by separating them from the residual aqueous phase through a double-step diethyl-ether (#32203-M Merck/Sigma-Aldrich) and acetone (#32201-M Merck/Sigma-Aldrich) extraction procedure (Procedure 1), carried out at ambient temperature. First, the reactor was washed with diethyl-ether (DEE), vacuum filtering the content over a Whatman glass microfiber filter ($1 \mu\text{m}$). Water and water-soluble organics (WSO) were then recovered by gravity separation, while DEE-soluble fraction (lighter biocrude, BC1) was obtained after rotary evaporation of DEE at reduced pressure. Finally, the reactor walls and the solids were washed with acetone (DMK) recovering a second biocrude fraction (BC2) and separating the solid residues (SR). A scheme representing the solvent extraction is depicted in Figure 1. Furthermore, a second and different procedure (Procedure 2) was also tested to evaluate the influence of the extraction method on compounds distribution. Here the aqueous phase was recovered before the solvent extraction step.

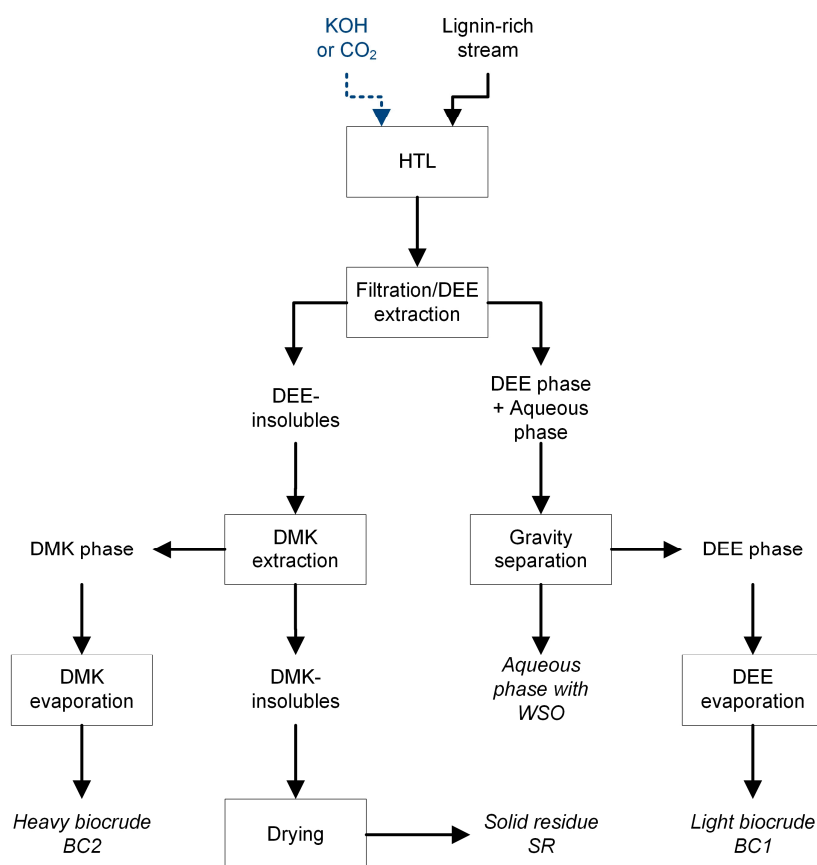


Figure 1. Extraction procedure for hydrothermal liquefaction (HTL) products recovery (Procedure 1).

For the additional tests with CO_2 , an overall molar ratio of $2.68\% \text{ molCO}_2/\text{molH}_2\text{O}$ was inserted in the reactor at 3 MPa and 25°C , substituting the Ar used for the uncatalyzed reactions and, at this initial condition, $1.83\% \text{ molCO}_2/\text{molH}_2\text{O}$ were dissolved into water.

2.3. Hydrothermal Reaction Conditions

The experimental campaign was first carried out by varying the reaction severity through temperature and residence time regulations. The ranges of reaction parameters were chosen within typical industrially viable limits. Residence time ranged respectively from 5 to 10 min and 10 wt. % of B/W, while three values were investigated for reaction temperature, 300–350–370 °C. The effect of base catalyzed reactions at 300 and 350 °C was also evaluated by adding KOH in a percentage of 2 wt. % and 4 wt. % relative to dry lignin sample. Hydrothermal reactions were also tested in the presence of an acid environment using supercritical CO₂ at 300 °C and the effect evaluated in comparison with KOH and in absence of catalysts.

2.4. Characterization of Liquid Products

Each hydrothermal liquefaction experiment was replicated at least two times. The aqueous phase (AP) was analyzed by quantifying the WSO content in HPLC. Before the injection, aqueous samples (25 µL) were first filtered through a 0.2 µm pore size syringe filters and quantitative analysis was carried out after a five levels calibration for each compound. Moreover, total organic carbon (TOC) analyses were carried out on aqueous phases samples by a TOC Cell Test Spectroquant®14879 (Merck) test kit and a Shimadzu UV-1800 spectrophotometer (605 nm). A Merck TR320 thermoreactor was used to heat the samples for 2 h at 120 °C and then cooled for 1 h in a test tube rack until reaching room temperature. The correction due to DEE contamination is reported in authors' previous work [26]. Qualitative and quantitative analysis of BC1 samples were carried out into a GC-MS apparatus: 0.1 g of BC1 samples were first dissolved in 10 mL of isopropanol and 2 µL of the solution were injected in a GC 2010 with a GCMS-QP2010 mass spectrometer (Shimadzu, Kyoto, Japan). The gas chromatograph was equipped with ZB-5 MS column (Phenomenex, Torrance, California, USA): 30 m length, 0.25 mm internal diameter and 0.25 µm film diameter. The temperature was initially set at 40 °C for 10 min, increased first to 200 °C (heating rate 8 °C min⁻¹, holding time 10 min) and then to 280 °C (heating rate 10 °C min⁻¹, holding time 30 min). Spectral interpretation was performed with NIST 17 database and the quantification was carried out through a 4-point calibration using o-terphenyl as internal standard. A complete list of calibrated compounds for GC-MS and HPLC quantification is given in Table S1 contained in the supporting information. In both the adopted analytical methods, the compounds detected below 25 % of the lowest calibration point concentration were considered as below limit of quantification and not taken in account. In addition, a comparison between the molecular weight (polystyrene equivalent) of the light and heavy biocrudes obtained by KOH-catalyzed reactions were evaluated by gel permeation chromatography (GPC). Tetrahydrofuran (THF) was used to dissolve biocrude samples, leaving the solution overnight. The solution was syringe-filtered at 0.45 µm and 100 µL were injected in an HPLC apparatus (Shimadzu LC 20 AT Prominence) with two in-series columns (Agilent, PL gel 5 µm 100 Å 300 × 7.5 mm), a guard column (Agilent, PL gel 5 µm 50 × 7.5 mm) a refractive index detector. The flow of the eluent (THF, 1 mL min⁻¹) was kept at 40 °C. Calibration was carried out with linear polystyrene standards (Agilent, 370–9960 g mol⁻¹).

The quantitative results were further referred to the dry feedstock mass, calculating the yields according to the equations below:

$$Y_x = Y_{BC1,x} + Y_{WSO,x} \quad (1)$$

$$Y_{BC1,x} = \frac{C_{GC,x} \cdot v_{GC}}{m_{l,db}} \cdot 100 ; Y_{WSO,x} = \frac{C_{HPLC,x} \cdot v_{HPLC}}{m_{l,db}} \cdot 100 \quad (2)$$

Where Y_x is the total yield of a x compound as sum of yields in BC1 ($Y_{BC1,x}$) and water soluble organics (WSO) in the aqueous phase ($Y_{WSO,x}$). While $C_{GC,x}$ and $C_{HPLC,x}$ are the concentrations in µg mL⁻¹ obtained in GC-MS and HPLC multiplied for the respective volumes of each phase (v_{GC} and v_{HPLC}). $m_{l,db}$ represents the mass of feedstock in dry basis employed in each experiment.

NMR analyses were carried out on BC1 and BC2 samples. Moreover, ^1H NMR spectra were recorded with a INOVA NMR 400 (Varian, Palo Alto, CA, USA) using dimethylsulfoxide- d_6 as solvent. Spectra were referenced to tetramethyl-silane. Solvent suppression was employed to record the spectra.

3. Results and Discussion

The hydrothermal conversion of LRS resulted in the generation of five main products: DEE-soluble biocrude (BC1), DMK-soluble biocrude (BC2), aqueous phase (AP) with water-soluble organics (WSO), char or solid residue (SR) and gases. The solvent extraction procedure was employed to maximize the recovery of biocrude fractions. In another work [26] the authors reported the results of the uncatalyzed experimental campaign only in terms of yields, elemental analysis and molecular weight: here, a detailed characterization of BC1 and AP was carried out to observe how the mechanism of lignin depolymerization is influenced by reaction conditions.

A detailed list of the resulting mass yields is presented in Table S2. The analyzed compounds were grouped in these chemical classes: Phenol (considered as a single compound), Methoxyphenols, Dimethoxyphenols, Catechols, Methoxycatechols, Phenolic Ketones, Phenolic Aldehydes, Acids, and Alcohols.

3.1. Lignin-Rich Stream Characterization

The lignin-rich feedstock was received in form of wet agglomerated particles with 69.7 wt. % of moisture content; therefore, it was dried, knife-milled, and sieved to < 0.25 mm prior to be used in the experiments. Carbon, hydrogen, nitrogen, and sulfur (CHN-S) and proximate analysis indicated the dry based composition to be 54.2 wt. % carbon, 5.9 wt. % hydrogen, 1.0 wt. % nitrogen, 0.2 wt. % sulfur, 36.1 wt. % oxygen (by difference), and 2.6 wt. % ash. Volatile matter and fixed carbon resulted to be respectively 71.0 wt. % d.b. and 26.4 wt. % d.b. The lignin content of the feedstock, together with its residual structural sugars is reported in Table 1 and the data are in good agreement with similar feedstock from enzymatic hydrolysis of lignocellulosic biomass investigated by Jensen et al. [13].

Table 1. Lignin and sugars content in LRS.

Parameter	Value [-] wt. % (d.a.f.)
Acid insoluble lignin	52.7 ± 4.99
Acid soluble lignin	0.253 ± 0.0216
Total lignin	53.0 ± 5.02
Structural sugars	35.8 ± 0.314
Glucan	30.7 ± 0.484
XMG*	4.94 ± 0.170
Arabinan	0.163 ± 0.0287

* Xylan, Mannan, Galactan.

The slurry of LRS in water was prepared at 10 wt. % of biomass to water ratio (B/W). The initial aqueous fraction of lignin-rich slurry was analyzed in HPLC to characterize the water-soluble content prior to the hydrothermal reactions, discriminating the compounds that were soluble at ambient conditions from those produced during the hydrothermal treatment. The total water-soluble HPLC-detectable content was about 4–5 wt. % (d.b.). The results, depicted in Figure S1 in the supporting information, showed the presence of a small percentage of dissolved sugars such as glucose and xylose-mannose-galactose (XMG) as well as glycerol, acetic and lactic acid. Lactic acid was the most abundant compound, deriving from bacterial contamination in the fermentation process. Indeed, lactic acid bacteria, which produces also acetic acid, can survive to typical fermentation conditions and represent the most common bacterial species found in ethanol facilities [29]. On the other hand, glycerol is known to be one byproduct of bioethanol production performed by yeasts, such as *Saccharomyces cerevisiae*, under aerobic and anaerobic growth condition [30].

3.2. Analysis of HTL Products

Typical chromatograms from GC-MS of BC1 and HPLC of AP are shown Figures 2 and 3, respectively, showing also chemical structures of the most present compounds. Moreover, Table S3 provides a complete light biocrude qualitative characterization with classes subdivisions for the same sample. HPLC chromatogram in Figure 3 depicts only the fraction of chromatogram containing organic acids and alcohols; however, this method was used to quantify also some phenolic compounds retained in the AP (Phenol; Phenol, 2-methoxy-; Phenol, 2,6-dimethoxy-; Phenol, 2-methoxy-4-methyl-; 1,2-Benzenediol and 1,2-Benzenediol, 3-methoxy-). A complete list of detected and quantified compounds in BC1 and AP is given in Tables S4 and S5, respectively in the Excel supporting information file.

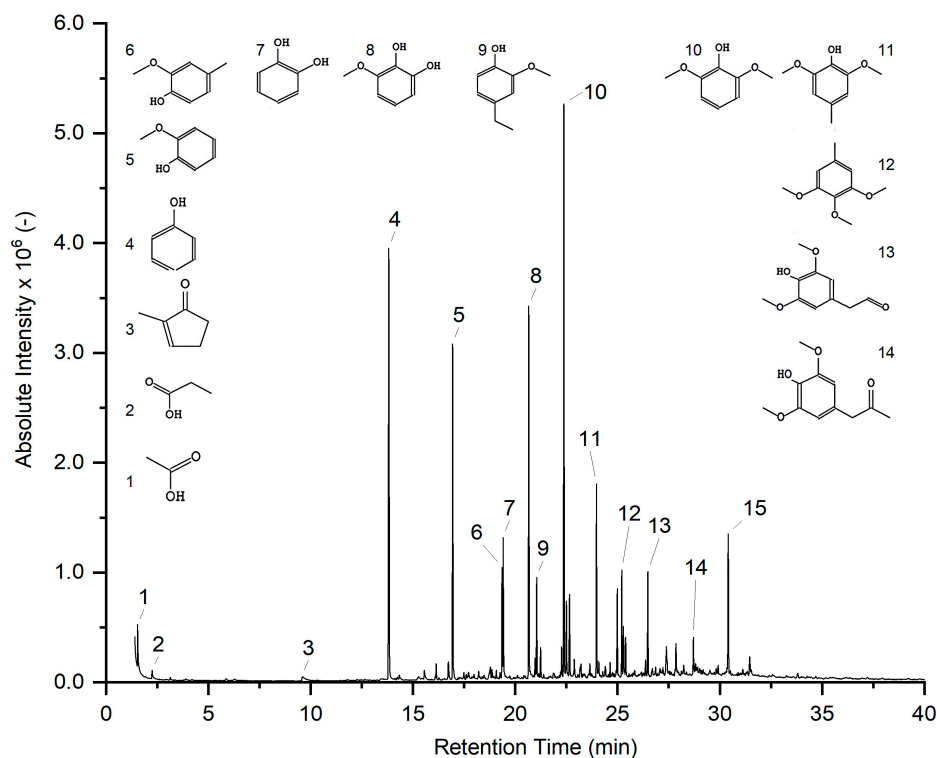


Figure 2. Typical GC-MS chromatogram for BC1 fraction obtained at 350 °C, 10 min, 10% biomass to water ratio. 1. Acetic acid, 2. Propanoic acid, 3. 1,2-Cyclopenten-1-one, 2-methyl-, 4. Phenol, 5. Phenol, 2-methoxy-, 6. Phenol, 2-methoxy-4-methyl-, 7. 1,2-Benzenediol, 8. 1,2-Benzenediol, 3-methoxy-, 9. Phenol, 4-ethyl-2-methoxy-, 10. Phenol, 2,6-dimethoxy-, 11. Phenol, 2,6-dimethoxy-4-methyl-, 12. Benzene, 1,2,3-trimethoxy-5-methyl-, 13. Homosyringaldehyde, 14. Syringylacetone, 15. o-Terphenyl (Internal Standard).

The degradation of the main biomass constituents under hydrothermal conditions have been extensively studied and reviewed [31,32]. The lignin three-dimensional matrix results from the interaction of three main aromatic structures (monolignols) named coniferyl, sinapyl, and p-coumaryl alcohols, which yielded aromatics constituents: guaiacyl (G), syringyl (S), and p-hydroxyphenyl (H) units. These monolignols are linked together in the polymeric structure through many different bonds such as ether (β -O-4, α -O-4, and 4-O-5) and C-C (β - β , β -5, and β -1) bonds [33,34]. During hydrothermal conversion reactions, the chemical bonds of the branched aromatic polymeric structure of lignin are broken to form phenolic monomers such as phenol, methoxyphenols, alkylphenols, dimethoxyphenols, catechols, methoxycatechols, phenolic aldehydes, and phenolic ketones [12,35,36]. In previous studies, it was observed that the ether bonds are more easily broken than C-C bonds, and this is the main depolymerization mechanism occurring in absence of catalyzed reactions [37]. The results from the present study confirmed that the reaction products from hydrothermal conversion

maintains the aromatic rings, while the substituent groups have different trends depending on reaction conditions. Indeed, in absence of catalysts, the main reaction occurring in aqueous environment at subcritical condition is known to be hydrolysis. Moreover, also, fragmentation and repolymerization occur during the liquefaction reaction mechanisms. Primary depolymerization products found in BC1 were Phenol, 2-methoxy (guaiacol) and Phenol, 2,6-dimethoxy- (syringol) coming from the thermal cleavage of guaiacyl and syringyl units as identified in peaks 5 and 10 in the GC-MS chromatogram in Figure 2. In addition, model compounds studies [38,39] showed that secondary reactions lead to the formation of catechol (peak 7), methoxycatechol (peak 8) and phenol (peak 4) through demethylation and demethoxylation giving rise to the methanol content in the AP, as detected through HPLC (Figure 3). Other lignin degradation products, which were detected by GC-MS, as reported in table S3 of the supporting information, are phenolic aldehydes and ketones, especially: Syringaldehyde (Benzaldehyde,4-hydroxy-3,5-dimethoxy-), Vanillin (Benzaldehyde,4-hydroxy-3-methoxy-), Acetovanillone (Ethanone,1-(3-hydroxy-4-methoxyphenyl)-), and Acetosyringone (Ethanone, 1-(4-hydroxy-3,5-dimethoxyphenyl)-). Due to the polarity of most of these compounds, a fraction of the oxygenated aromatic substances (mostly phenol, guaiacol, and syringol) was also found trapped in AP after the solvent extraction procedure.

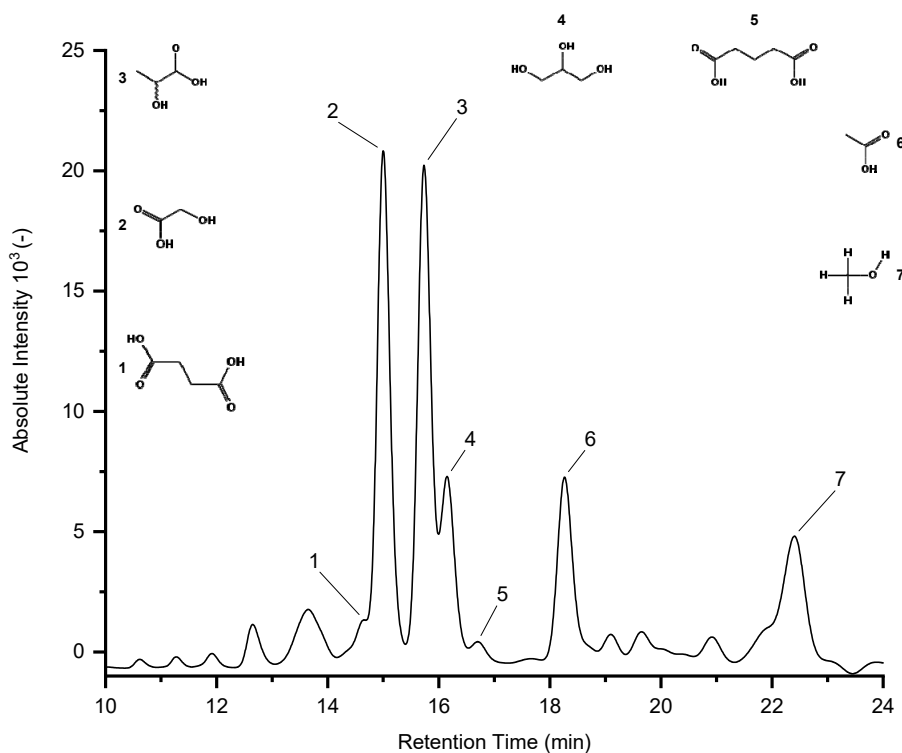


Figure 3. Typical partial HPLC chromatogram for water-soluble organics (WSO) in aqueous phase (AP) fraction obtained at 350 °C, 10 min, 10% biomass to water ratio. 1. Succinic acid, 2. Glycolic acid, 3. Lactic acid, 4. Glycerol, 5. Glutaric acid, 6. Acetic acid, 7. Methanol.

The polysaccharides contained in the feedstock adopted for lignocellulosic ethanol production were already subject to depolymerization during hydrolytic pretreatment in the ethanol production process (steam explosion and enzymatic hydrolysis), right before fermentation [40,41]. In HTL, cellulose, hemicellulose, and derived sugars (e.g., glucose or fructose) are mainly converted into organic acids, alcohols and ketones during hydrolysis reaction [42–44]. As known, acid and alcohols have higher affinity with water and therefore were mostly found in the aqueous phase, as reported in the HPLC chromatogram of the residual aqueous phase in Figure 3. Acetic acid and formic acids are formed by degradation of glucose in alkaline and neutral conversion. Even though acetic and lactic

acid can potentially be produced during hydrothermal reactions, they were also already found in the feedstock slurry thus meaning that they were mainly produced and dissolved in water during ethanol fermentation in the upstream production plant and not only during hydrothermal reactions [40,45]. It was also confirmed that reaction of sugars in hydrothermal media leads to the generation of cyclic ketones (e.g. cyclopentenones) and their alkylated forms, as already proposed in literature [46].

It was not possible to analyze heavy molecular weight compounds comprised in BC2 using GC-MS or HPLC. The heavier fraction still contains oligolignols generated in the first depolymerization steps as well as repolymerization of lignin fractions [47]. Thus, we were unable to characterize the composition of BC2 with these analytical techniques, but representative infra-red spectra and molecular weight-average distributions of BC1 and BC2 were already given in a previous work [26], showing similarities with the lignin feedstock and demonstrating the higher average molecular weight of BC2, ranging from 1030 to 1400 g mol⁻¹. Therefore, BC2 was supposed to be completely composed by lignin-oligomers not converted to lighter compounds (e.g., phenolic monomers). Here, to further characterize the biocrudes, ¹H NMR analysis was carried out on BC1 and BC2 derived from reaction at 370 °C and 5 min of residence time, comparing the resulting spectra with literature data. ¹H NMR spectra reported in Figure 4 show typical depolymerized lignin signals in light and heavy biocrude fractions [11,48–51]. The signals in the 8–10 ppm region, ascribable to phenolic OH [48,49], are slightly visible only in BC1 and probably due to the cleavage of the β-O-4 bonds. The region between 6–8 ppm indicates the aromatic protons and unsaturated aliphatic bonds (C=C) signals typical of the lignin oligomers and primary lignin monomeric units, confirming the aromatic ring and β-double bonds preservation in both BC1 and BC2 samples [48,50]. Both biocrude fractions also denote the presence of peaks in chemical-shift range 3–4 ppm related to methoxy groups (–OCH₃) as confirmed by literature data [52,53]. The 1.5–3 ppm protons are typically assigned to –CH₃ and –CH₂- bonded to aromatic structures [54] and signals are visible in both fractions. In the 0.5–1.5 ppm region, aliphatic protons typical of methyl and methylene groups are more defined in BC2, suggesting an ineffective hydrolysis of C–C lignin bonds [37,52]. To sum up, ¹H NMR confirmed the incomplete depolymerization of lignin structures and no conspicuous differences were found in the functional groups of the two biocrudes due to the similar nature of the structural oligolignols constituents.

In the next sections, the trend of detected monomeric LRS-derived fractions in function of the reaction conditions will be analyzed to further characterize the hydrothermal depolymerization process.

3.3. Hydrothermal Liquefaction in Absence of Catalysts: Influence of Temperature and Time

The results from hydrothermal liquefaction of lignin-rich streams shows an effective depolymerization into more valuable products, even in absence of catalyzed reaction. These results have been used to optimize the process conditions prior to test the effect of catalytic additives.

The effect of temperature in non-catalytic condition was evaluated carrying out HTL tests at 300–350–370 °C with 5 minutes of residence time and 10 wt. % of B/W. Yields of compounds versus dry feedstock, evaluated according to Equation (1), are shown in Figure 5. First, higher temperatures enhance the production of aromatic monomers from lignin. Catechols content linearly increased and their methoxylated forms were almost absent at low temperature, appearing only at 350 °C. Similar trends were observed for methoxyphenols, dimethoxyphenols, and phenol. However, a lower or absent increment-rate at temperature between 350–370 °C was noticed. Moreover, the yield of phenolic carbonyls zeroed passing from 300 °C to 350 °C, suggesting the high reactivity of the carbonyl substituent that leads to the formation of simpler monomers. The same effect was observed for cyclopentenones.

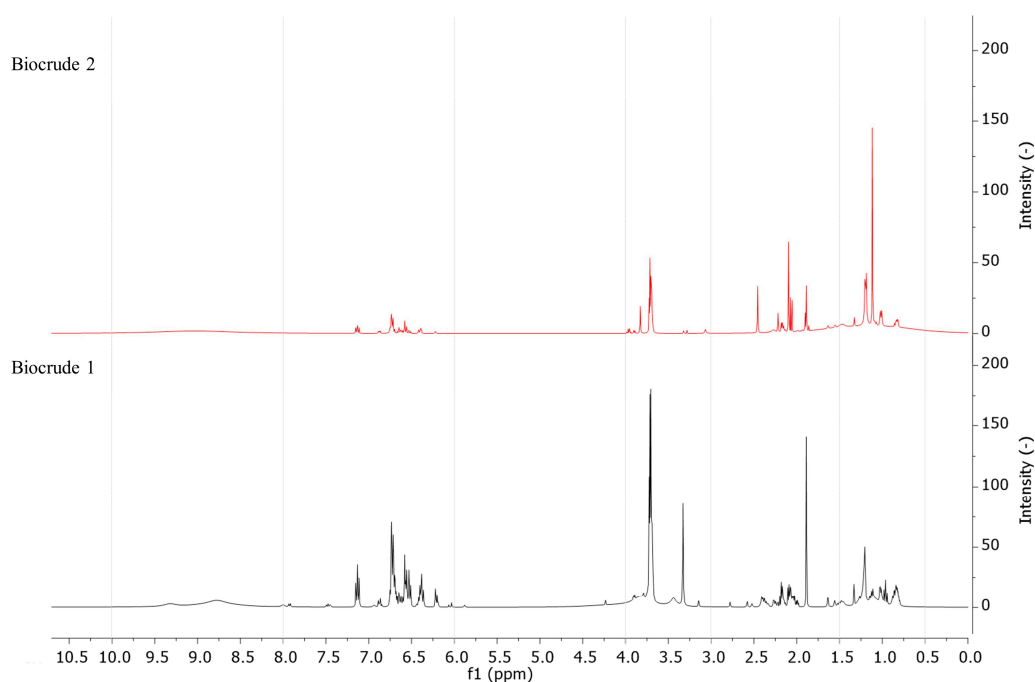


Figure 4. ^1H NMR spectra for DEE-soluble biocrude (BC1) and DMK-soluble biocrude (BC2) from test at 370 °C and 5 min.

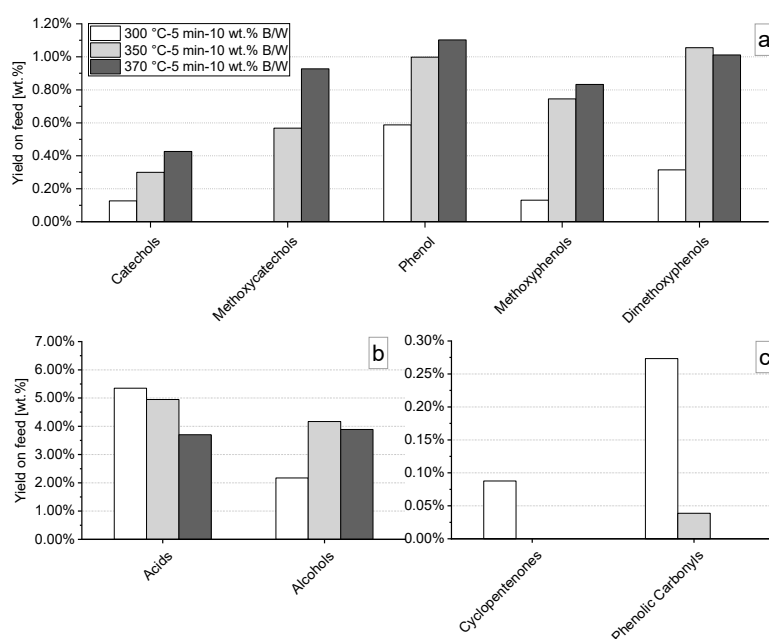


Figure 5. Effect of reaction temperature on yields of quantified compounds for uncatalyzed HTL tests: (a) phenolics, (b) acids and alcohols, (c) phenolic carbonyls and cyclopentenones. When no graph column is depicted, the concentration was below quantification limits.

It was also observed that an increment in the reaction temperature caused a considerably high decrement in the acids yield, from 6 wt. % at 300 °C to less than 4 wt. % at 370 °C. This is mainly due to the degradation of lactic acid while acetic and glycolic acid formation remained more stable, as depicted in Figure 6a. In addition, the difference plot in Figure 6b shows a comparison between the acids already contained in the initial slurry at ambient conditions and the acids content after the reaction. Glycolic acid was always generated during liquefaction reactions as it was not identified in

the initial slurry. Acetic acid instead was partially produced, while lactic acid was always cracked during the conversion process and it was not generated during the reactions. The rate of lactic acid degradation increased at higher temperature and, as other authors suggests [55], the fragmentation reaction forms mainly light gases like CO, CO₂, and CH₄. The gas yield was theoretically evaluated from initial and final reactor pressure, by assuming only CO₂ as gaseous specie and by considering the ideal gas law; results are reported in Table S2. Benzoic acid has a similar trend as phenolic carbonyls compounds, and its presence in the resulting liquids was reduced at higher temperature (Figure 6a). The analysis on the AP showed that the alcohols produced are mainly methanol and glycerol. Methanol content seemed to be highly influenced by the temperature (Figure 6a) while glycerol, already presents in the LRS slurry, was cracked during the reactions (Figure 6b). As explained before, the effect of higher temperature in the reaction zone promotes the depolymerization of the lignin structures, including the loss of the methoxy group from the fragmentation of the methoxyphenols and dimethoxyphenols. The availability of free methoxy substituents in the subcritical environment gives rise to the formation of methanol through demethylation reactions. This mechanism is enhanced by temperature: an increase in reaction temperature leads to higher rate of formation of free radicals from lignin cracking, as the formation of methoxyphenolic compounds raised together with the enhanced cracking into catechols and phenol. To sum up, the reaction temperature had a strong effect on BC1 monomers and WSO yield, especially in the range 300–350 °C. Moreover, even though moving close to critical condition, i.e., 370 °C, could have a positive effect on depolymerization and WSO reduction (see mass yields in Table S2), the overall process costs would increase in a scale-up perspective. For this reason, a temperature of 350 °C was selected in the following experiments, where the influence of residence time was evaluated.

The reaction mechanisms of the HTL process also depends on the residence time of the feedstock at the reaction condition with water at subcritical state. The latter is indeed a very important parameter and should be kept as low as possible, as in a continuous scaled-up perspective, it influences the size of the reactor and, consequently, the throughput of the plant. Moreover, other studies [56,57] already reported that an increment in the residence time would favor condensation and repolymerization reactions increasing the yield of heavy biocrude and solid residues. Thus, a fast cooling step is needed to quench the reactions and partially avoids further polymerization of lignin intermediates. Therefore, in agreement with literature, we decided to investigate rather short residence times, from 5 to 10 minutes at 350 °C (Figure 7). As also found by other authors [58,59], during HTL reactions in subcritical water, methoxylated phenols cleavage rate increases with reaction time, leading to a higher amount of catechols in the product (e.g., 1,2 Benzenediol from Phenol, 2-methoxy-). In agreement with them, in this work, a small increment in the yields of catechols and methoxycatechols was observed together with a reduction of methoxyphenols yields in the range 5–10 minutes. Phenol yield was reduced at higher time due to the fact that catechols formation is always the preferred reaction route from methoxyphenols cleavage in subcritical water conditions, meaning that phenols undergo to substitution reactions more rapidly than catechols [60]. Regarding the acids content in the liquid products, a higher residence time slightly reduced the overall yield due to the enhanced cracking rate, leading to the formation of light gases, as confirmed by the gas yield increase from 4.5 to 5.5 wt. % (see Table S2). This is due to the enhanced cracking of lactic acid from the feed and to the degradation of the produced acetic and glycolic acids. The generation of alcohols remained constants, probably due to an equilibrium between the cleavage of alcohols functional group from lignin cracking and the consequent enhanced volatilization. The phenolic carbonyls completely crack with higher reaction time, meaning that a complete hydrolysis of the carbonyl substituent groups is achieved in the investigated residence time.

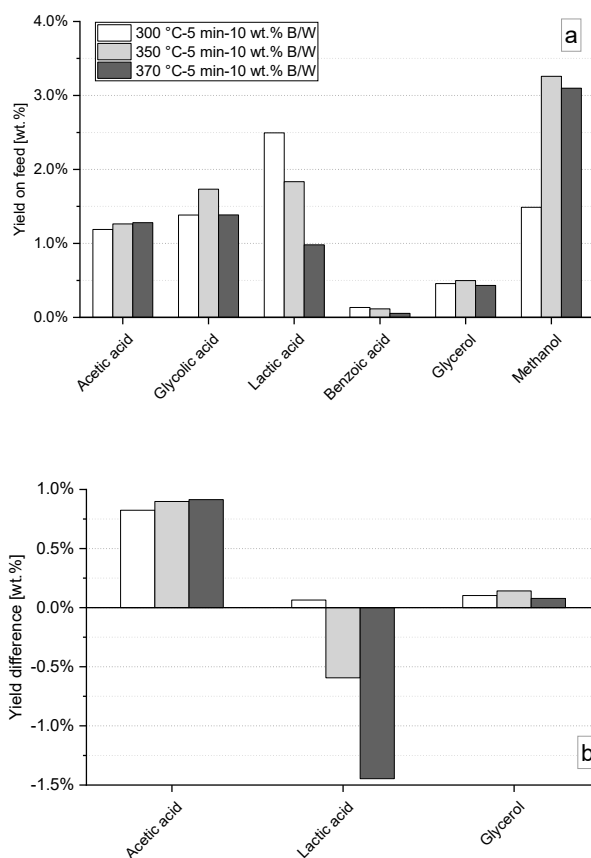


Figure 6. (a) Effect of reaction temperature on yields of specific acids and alcohols species; (b) difference plot for acids degradation versus formation compared to the initial acids content in the lignin-rich streams (LRS) slurry for uncatalyzed HTL tests.

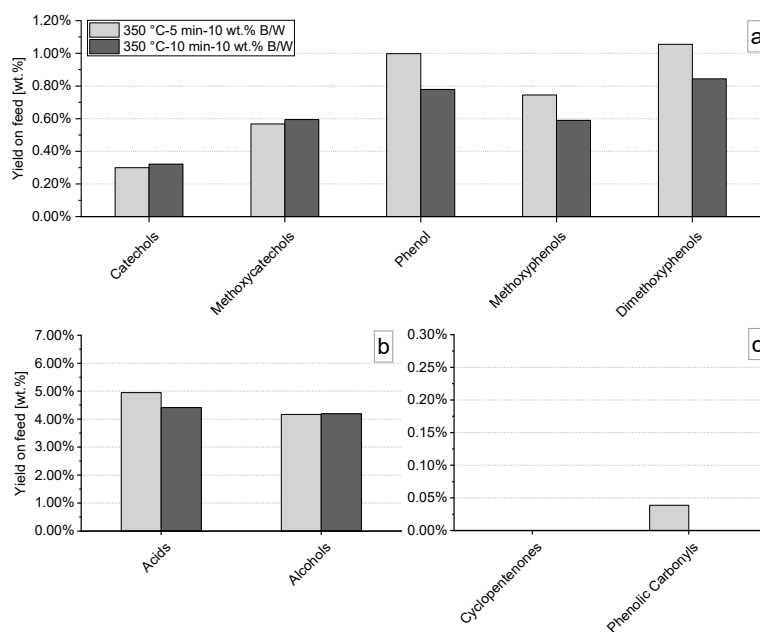


Figure 7. Effect of residence time on yields of quantified compounds for uncatalyzed HTL tests: (a) phenolics, (b) acids and alcohols, (c) phenolic carbonyls and cyclopentenones. When no graph column is depicted, the concentration was below quantification limits.

3.4. Influence of Catalytic Additives in the Process

The effect of additives with catalytic effect was evaluated as a method to improve the liquefaction process. First, base catalyzed reactions were carried out by varying the reaction temperature and comparing the results to those obtained in absence of alkaline hydroxides catalysts. In addition, the catalytic effect of supercritical carbon dioxide (sCO₂) was tested comparing the effect at lower reaction temperature, substituting the Ar inside of the tubular reactor.

3.4.1. Effect of pH Control Using Strong Basis

Base catalyzed depolymerization was realized adding KOH in the slurry mixture, at 2 and 4 wt. % of KOH to LRS ratio dry basis, obtaining an initial slurry pH of 8.0 and 10.0 respectively, doubling the baseline value as reported in Table 2.

Table 2. pH values of feed and products with and without KOH. Test performed at 350 °C, 5 min, and 10 wt. % biomass to water ratio (B/W).

Stream	pH of Control	pH @ 2 wt. % KOH	pH @ 4 wt. % KOH
feed	4.6	8.0	10.0
AP	4.4	5.1	5.8

When reactions occurred in alkaline condition, the overall biocrude mass yield (BC1 + BC2), measured by weighting each resulting phase, increased at lower temperature (300 °C) from 48.8 wt. % to 55.3 wt. % when 2 wt. % of KOH was used, as summarized in Table 3. On the contrary, increasing the reaction temperature to 350 °C the total biocrude mass yield was reduced from 59.0 wt. % in absence of KOH to 54.0 wt. % and 53.2 wt. % when 2 wt. % and 4 wt. % of KOH were tested respectively. A further increment in the temperature (370 °C) confirmed the same trend. However, high initial pH had an overall positive effect increasing on lighter biocrude fraction (BC1) resulting in higher mass yields at each temperature tested. On the other hand, heavier BC2 yield was always reduced, especially in the range 350–370 °C. Hence, although the total biocrude yield was found decreased in basic conditions, higher amount of lighter lignin-derived compound was measured. Moreover the WSO content in the residual AP increased when final higher pH was achieved, in agreement with Belkheiri et al. [16]. TOC analysis (corrected subtracting the carbon contained in the water-dissolved DEE), reported in Table 4 shows an increment in the concentration of soluble organics in residual AP. At 350 °C the carbon concentration of WSO varied from 6648 to 8823 and 10,981 mg l⁻¹ increasing the initial slurry pH from 4.6 to 8 and 10 respectively. Similar effects were observed also at 370 °C. Moreover, as can be deduced from Table 4, the WSO carbon concentration, calculated from HPLC detectable data, diverge from the TOC value when higher depolymerization rate is reached, (i.e., at higher temperature and in alkaline conditions) and this is probably due to the higher concentration of undetected oligomeric compounds.

Molecular weight (or molar mass) was evaluated by gel permeation chromatography (GPC) and the average results for BC1, BC2 and the total biocrude (BC tot) were compared with KOH-catalyzed tests at 300 °C and 350 °C (Figure 8). The Mw of the total biocrude was determined as a yield-based weight-average from that of BC1 and BC2. The strong alkaline environment improved BC1 yield over BC2, consequently the resulting BC2 molecular mass increases. These results are in accordance with the fact that the increased rate of depolymerization leads to higher quantity of BC1 leaving in BC2 only heavier compounds. A confirmation can be found observing the total biocrude molecular mass (line in Figure 8) that it is always reduced when KOH is used. Therefore, an increment in the amount of KOH from 2 wt. % to 4 wt. % resulted in a higher depolymerization rate as confirmed by lower BC2 yields, plus a reduction of the total biocrude average molecular weight.

Table 3. Effect of base catalyzed reaction increasing KOH to LRS ratio from 2 wt. % to 4 wt. % at 300–350–370 °C, 5 min and 10 wt. % B/W: mass yields of light biocrude (BC1), heavy biocrude (BC2), solid residues (SR), Gas, and water-soluble organics (WSO) + loss. Absolute standard deviation is reported in brackets.

Temp. [°C]	KOH [%]	BC1	BC2	SR	Gas	WSO + Loss *
300	-	9.8% (1.6%)	38.8% (11.5%)	16.5% (3.0%)	2.4% (0.7%)	32.6% (10.5%)
	2	18.8% (0.7%)	36.5% (2.6%)	13.5% (0.7%)	2.2% (n.d.)	29.0% (2.6%)
350	-	27.0% (6.7%)	32.0% (6.4%)	11.4% (0.9%)	4.5% (0.8%)	23.8% (5.4%)
	2	37.0% (1.4%)	17.0% (0.5%)	10.2% (0.7%)	4.4% (0.6%)	31.3% (1.1%)
	4	35.5% (2.1%)	17.7% (1.4%)	9.3% (0.5%)	2.2% (0.3%)	35.4% (0.6%)
370	-	36.8% (1.7%)	15.8% (3.1%)	13.0% (0.9%)	4.0% (0.1%)	30.3% (2.3%)
	2	39.2% (0.5%)	9.7% (1.9%)	12.3% (0.0%)	4.3% (0.1%)	34.5% (2.0%)

* calculated by difference, n.d.: not determined.

Table 4. Total organic carbon (TOC) concentration of WSO, influence of KOH at 300–350–370 °C. Compared to carbon concentration calculated by HPLC detected compounds. Test performed at 5 min and 10 wt. % B/W.

Temp. [°C]	KOH [wt. %]	TOC—Concentration [mg l ⁻¹]	C—HPLC Detected WSO Concentration [mg l ⁻¹]
300	-	4741	3405
	2	5310	3859
350	-	6648	3186
	2	8823	3337
	4	10,981	4707
370	-	5937	5608
	2	8692	4513

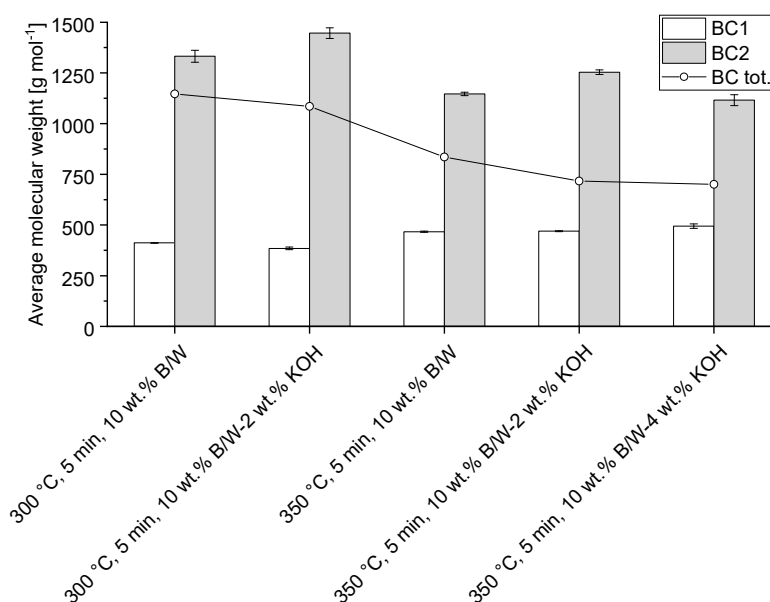


Figure 8. Effect of base catalyzed reaction, increasing KOH to LRS ratio from 2 wt. % to 4 wt. %: average molecular weight of BC1, BC2, and total biocrude. Error bars represent absolute standard deviation.

Looking at the monomeric compounds production, the results in term of yield of detected compounds are summarized in Figure 9 at constant reaction temperature (350 °C), time (5 min) and B/W

(10 wt. %). Increasing the pH of the initial slurry solution from 4.6 to 8.0, corresponding to an increment from no KOH to 2 wt. % of KOH to LRS ratio, a slight enhancement in the formation of phenolics species was observed, especially the methoxylated forms (i.e. methoxyphenols and dimethoxyphenols). Phenol yields were slightly increased with 2 wt. % of KOH but decreased again adding more KOH in the slurry. Regarding the catechols, the yield remained almost constant increasing the pH of the slurry but methoxycatechols yield was enhanced. The average acids yield was not significantly affected by the basic environment. Indeed, an increase of pH negatively affected the cracking of lactic acid, thus increasing its yield from 1.84 wt. % to 2.60 wt. % while the generation of glycolic acid was inhibited from 1.73 wt. % to 1.22 wt. % when initial slurry pH was 4.6 and 10.0 respectively. Alcohols production increases by adding higher amount of KOH, due to the already discussed effect on the overall enhanced depolymerization rate. In other words, the increment in BC1 yields can be correlated to the formation of a higher amount of methanol due to the demethylation and demethylation of the methoxy groups during the cleavage of the lignin methoxyaromatic building blocks. As regards to phenolic carbonyls species, the presence of base catalyzed reaction reduced the presence of this compound class below instruments calibration limits, meaning that the carbonyl branches were cracked to form other phenolic monomers (e.g., methoxyphenols) during catalyzed hydrolysis reactions.

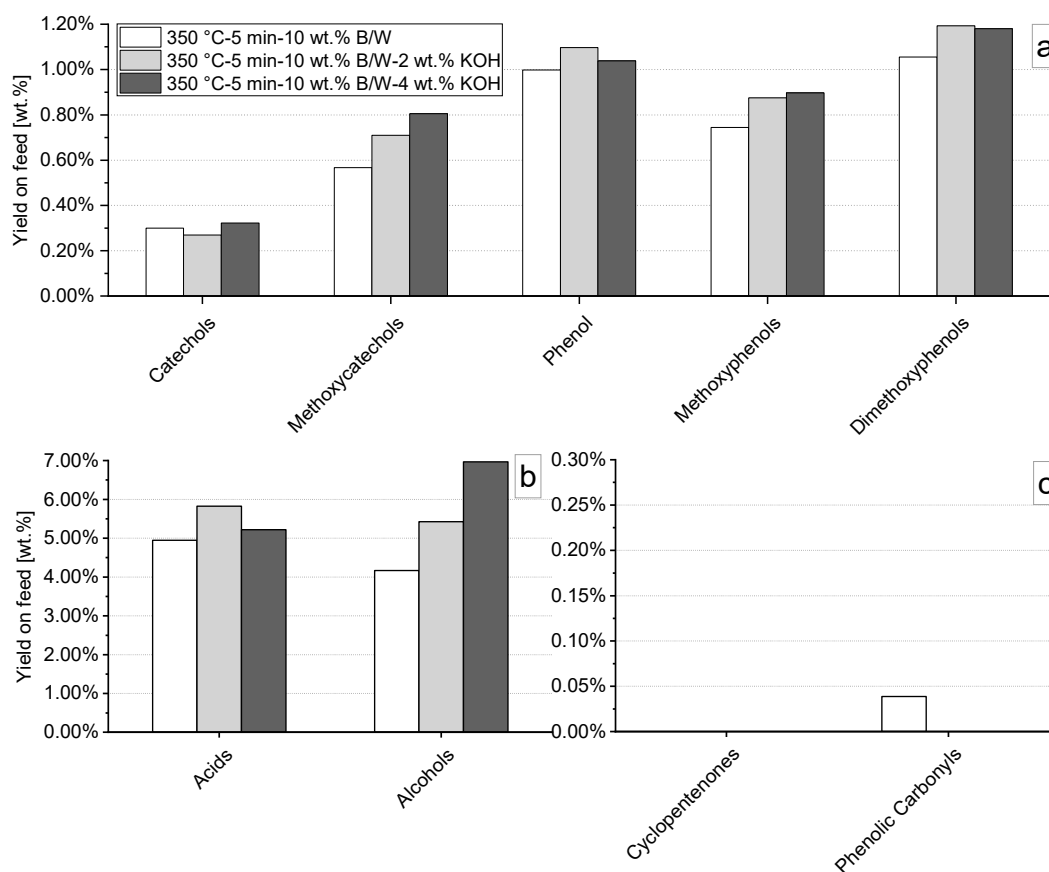


Figure 9. Effect of base catalyzed reactions increasing KOH to LRS ratio from 2 wt. % to 4 wt. % on yields of quantified compounds: (a) phenolics, (b) acids, and alcohols, (c) phenolic carbonyls and cyclopentenones. When no graph column is depicted, the concentration was below quantification limits.

3.4.2. Effect of Supercritical CO₂

The effect of supercritical CO₂ was tested in a biphasic mixture together with subcritical water in order to investigate the selectivity of specific monomers during the depolymerization of the biorefinery lignin-rich material. Other previous literature works demonstrated that sCO₂ can be used to enhance the selectivity towards the formation of specific phenolic compounds such as guaiacol during the

depolymerization of alkali lignin [61]. Carbon dioxide become supercritical above 31.1 °C and 7.39 MPa and its catalytic effect was evaluated in an HTL experiment carried out at 300 °C, 5 min residence time and 10 wt. % B/W. As in the reference experiment, with inert Ar atmosphere, the reactor was initially pressurized at 3 MPa, but the maximum obtained pressure (8 MPa) was lower of about 5 MPa, denoting higher dissolution rate of CO₂ compared to Ar. At the considered reaction temperature the percentages of dissolved moles of CO₂ increased, reaching a theoretical value of 2.9 molCO₂/molH₂O as other author suggests [61–63]. In this work the effect of CO₂ was evaluated in comparison to the results obtained in absence of catalysts and with KOH base catalyzed depolymerization. The results showed that, compared to the uncatalyzed case, the light biocrude yield increased, but the other mass yields were only slightly affected by the presence of supercritical carbon dioxide, meaning that the overall depolymerization rate is not influenced by the presence of sCO₂, as summarized in Table 5.

Table 5. Effect of CO₂ acid catalyzed reaction compared to base catalyzed and control test at 300 °C, 5 min and 10 wt. % B/W: mass yields of BC1, BC2, SR, Gas, and WSO + loss. Absolute standard deviation is reported in brackets.

Temp. [°C]	Catalyst	BC1	BC2	SR	Gas	WSO + Loss *
300	-	9.8% (1.6%)	38.8% (11.5%)	16.5% (3.0%)	2.4% (0.7%)	32.6% (10.5%)
300	2 wt. % KOH	18.8% (0.7%)	36.5% (2.6%)	13.5% (0.7%)	2.2% (n.d.)	29.0% (2.6%)
300	sCO ₂	15.5% (5.0%)	38.1% (8.2%)	16.2% (0.7%)	3.3% (n.d.)	26.9% (2.56%)

* calculated by difference, n.d.: not determined.

Even though the mass of depolymerized material was almost constant, the synergetic effect of sCO₂ together with subcritical water was highlighted by an enhanced generation of phenol, methoxyphenols and dimethoxyphenols compared to the results in absence of catalysts, as reported in Figure 10. Similar catalytic effect has been explained by Numan-Al-Mobin et al. [24], observing that sCO₂ in hydrothermal medium acts like acid homogeneous catalyst promoting the selectivity towards phenolic compounds. Compared to other homogeneous catalysts, the use of fluids at supercritical state with catalytic effects, like carbon dioxide, reduces the mass transportation limitations due to diffusivity and lower density that permits a higher penetration in the feedstock's pores. As a result, in our study, the phenolics yields obtained with supercritical carbon dioxide at 300 °C (1.10 wt. %) was comparable to the yields achieved in absence of catalyst or with 2 wt. % of KOH at higher reaction temperature (350 °C). Catechols and methoxycatechols yields were not affected by the presence of sCO₂, confirming the catalytic selectivity towards monohydroxy benzenes species (e.g., phenol, methoxyphenols and dimethoxyphenols), as also confirmed by the larger presence of phenolic carbonyls (mostly vanillin and syringaldehyde) in the liquid products. However, the methanol yield remained unvaried, therefore demethylation was not enhanced by the presence of sCO₂, confirming a stable depolymerization efficiency at 300 °C compared to the control test. In addition, a higher yield of cyclopentenones (e.g. 1,2-Cyclopentanedione, 3-methyl-) was observed when sCO₂ was injected in the process, this is probably due to an effective repolymerization or cracking inhibition of also sugars-derived compounds.

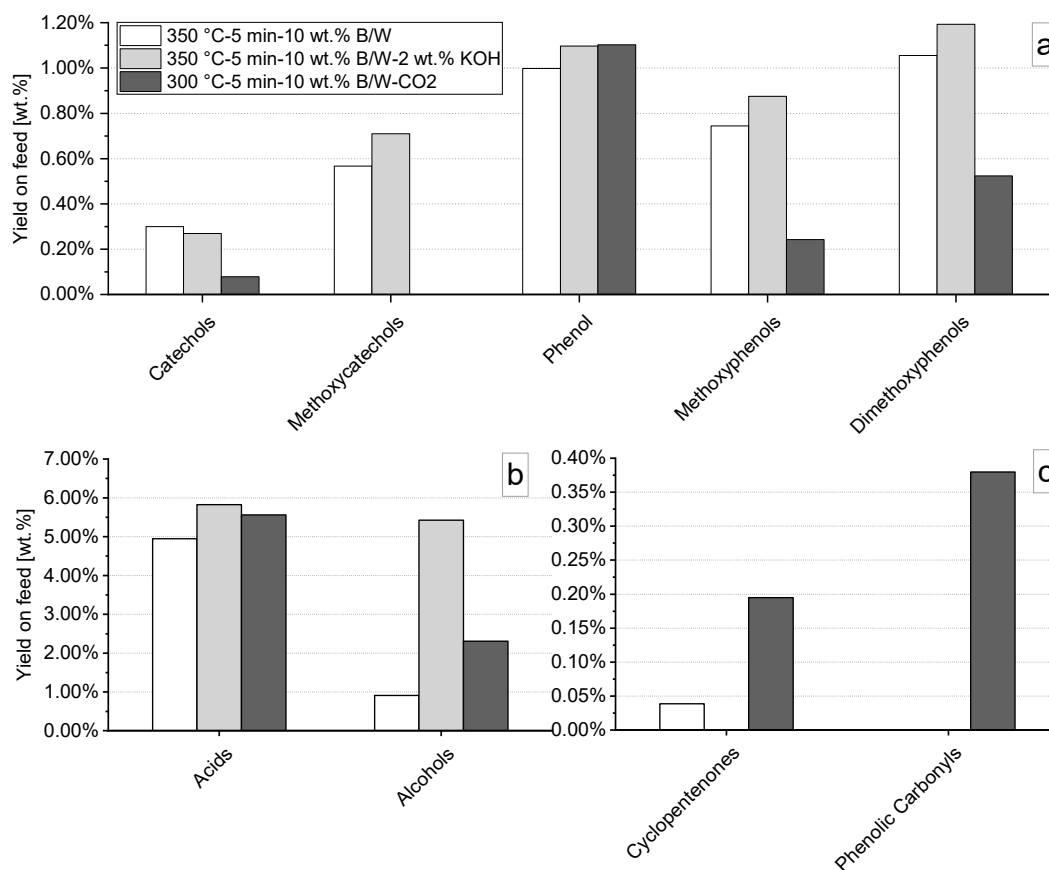


Figure 10. Effect of CO₂ acid catalyzed reaction compared to base catalyzed and blank tests on yields of quantified compounds: (a) phenolics, (b) acids and alcohols, (c) phenolic carbonyls, and cyclopentenones. When no graph column is depicted, the concentration was below quantification limits quantification limits.

3.5. Compound Distribution among HTL Fractions: Influence of Biocrude Extraction Procedures

In the previous sections a detailed discussion on the depolymerization of LRS in subcritical water, with and without the use of heterogeneous catalysts, has been presented without considering how the detected compounds are distributed among the resulting fractions. It is important to note that the products collection procedure have a strong effect on the detectable organic content of both BC1 and AP, due to differences in the sample composition analyzed. Complex chemical and thermodynamic equilibrium reactions are involved during the solvent extraction due to the presence of a multitude of different organic compounds in the aqueous, oily and solid HTL products. The use of a procedure rather than the other can have more than one justification. In this lab-scale work, Procedure 1 (described in Figure 1) was chosen to maximize the organic collection in the biocrude but, at larger scale, there could be the possibility to directly separate the oily fraction from the aqueous solution only with physical techniques (e.g., centrifugation or gravimetric separation). For this reason, a different test at the same HTL conditions (350 °C, 10 min, 10 wt. % B/W, no catalysts) was carried out recovering the aqueous solution directly after the reaction removing the DEE-extraction step on the aqueous phase (Procedure 2). The whole data set discussed before was obtained using the Procedure 1. With this method, the solvent (DEE) was directly put in contact with the HTL liquid and solid products, therefore maximizing the organic extraction in the BC1. As depicted in Figure 11, substantial differences in the product distribution have been identified when the aqueous solution was collected prior to the DEE extraction (Procedure 2). In this case, the solvent was not able to recover part of the organics in the biocrude, leaving some molecules in the AP as WSO.

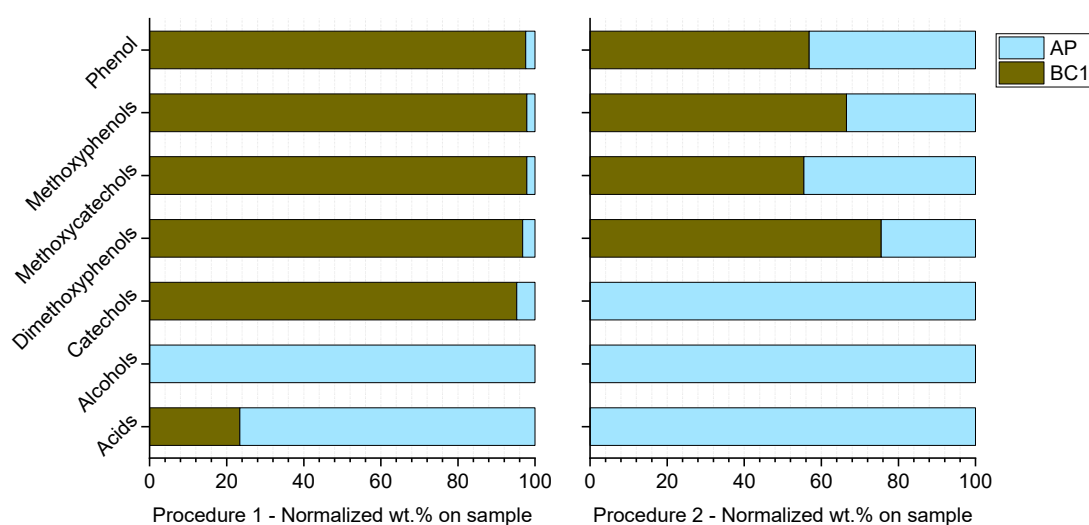


Figure 11. Influence of collection procedures on organic compounds distribution among BC1 and AP fractions. Tests performed at 350 °C, 10 min, 10 wt. % B/W in absence of catalysts.

As regards the normalized distributions in Figure 11, the collection of phenolics in the BC1 is highly reduced (about 20–30 %) when Procedure 2 was tested. Same results were observed for the methoxycatechols, whereas the catechols (mostly 1,2 benzenediol) remained totally trapped in the AP without getting recovered as DEE-soluble. Part of the carboxylic acids were recovered as DEE-soluble with Procedure 1 (mostly acetic acid) but when the aqueous phase was recovered directly after the reactions, the whole acid content remained in the AP, given the high affinity with water. On the other hand, the collection methodology did not have any effect on the alcohols distribution since the solvent was not able to extract these compounds. Thus, the collection procedure must be carefully considered for adequate comparisons of results as well as for the implementation of these types of procedures in an industrial scale-up perspective. Moreover, the implication of different extraction procedures will impact on possible downstream aqueous phase valorization steps such as aqueous phase reforming [64] or other valorization routes for chemicals extraction [65,66].

4. Conclusions

Lignin-rich streams (LRS) from a demo-scale lignocellulosic ethanol plant was successfully depolymerized in subcritical water varying three main process parameters, such as temperature, time, as well as introducing KOH and sCO₂ as catalysts for process optimization. Even though temperature was found to be the most influent parameter increasing the LRS depolymerization efficacy at the experimental conditions investigated in this work, the effect of time and B/W was evaluated in order to observe differences in the detected monomeric products yields into BC1 and AP. Regarding residence time, 5 minutes were sufficient for lignin and sugars cleavage in subcritical water, while the increase to 10 minutes eventually promoted substitution and repolymerization reactions, leading to a reduction in methoxyphenols contents while keeping constant the catechols content. Temperature was demonstrated to play a fundamental role in the hydrothermal reaction mechanisms, and a T increase from 300 to 370 °C caused an enhanced phenolic monomer content in BC1 and AP, together with a reduction of AP acids content. However, increasing the temperature closer to water critical point (374 °C, 22 MPa) will also increase the CAPEX of a scaled plant, due to higher equipment costs related to materials resistance at these severe operation conditions, however at sufficiently high pH of the liquid medium the corrosion effects on metals will be reduced. Thus, the use of an alkaline slurry solution is a preferable route at higher temperature [67]. Moreover, the use of KOH as alkaline homogeneous catalyst resulted in an improved overall LRS depolymerization, as observed by the enhanced overall BC1 mass yield and WSO content as well as a reduction in the average molecular weight of the total

BC. On the other hand, the presence of KOH did not enhance the formation of phenolic monomers, but the higher yield of methanol in the aqueous solution confirmed the positive effect on lignin structure cleavage. CO₂ as acid catalyst showed interesting phenolics-selective properties at his supercritical state, when tested in a biphasic solvent mixture with subcritical water. Comparing acid (sCO₂) to base catalyzed depolymerization (with KOH), similar phenolic yields were generated at low temperature (300 °C). The phenolics fraction produced with sCO₂ was also comparable to the one obtained at 350 °C with and without KOH. Therefore, although the introduction of sCO₂ as acid catalyst into the process had not significant effects on the overall BC yields, it showed an enhanced selectivity on the formation of phenol and methoxyphenols monomers in the products at lower temperature compared to the uncatalyzed control test. Moreover, the influence of the collection procedure has been presented and discussed in order to demonstrate the different composition of BC1 and AP when a physical separation step is interposed before a chemical solvent extraction.

Supplementary Materials: The following are available online at <http://www.mdpi.com/1996-1073/13/5/1241/s1>, Figure S1: Water-soluble compounds in LRS liquid fraction of the slurry: yield on feed at 10 wt. % and 20 wt. % of B/W, Table S1: Compounds calibrated in GC-MS and HPLC, Table S2: Yields of the HTL products from all investigated reaction conditions. Absolute standard deviation is reported in brackets, Table S3: Qualitative analysis of a light biocrude sample produced at 350 °C, 10 min, 10 wt. % (procedure 1), Table S4: GC-MS - light biocrude (BC1), Table S5: HPLC - aqueous phase (AP).

Author Contributions: Conceptualization, A.M.R.; Formal analysis, S.D.O., E.M., and G.L.; Investigation, S.D.O., E.M., and G.L.; Methodology, A.M.R., E.M., S.D.O., and D.C.; Supervision, D.C.; Validation, A.M.R. and D.C.; Visualization, S.D.O.; Writing—original draft, S.D.O.; Writing—review & editing, E.M., A.M.R., L.R., and D.C. All authors have read and agreed to the published version of the manuscript.

Funding: This study was partly funded by the European Union’s Horizon 2020 research and innovation program, project Heat-to-Fuel, under Grant Agreement number 764675.

Acknowledgments: The authors intend to acknowledge Alberto Bini for his contribution in performing the HTL experiments, TOC analyses, data collection, and Lorenzo Bettucci for his contribution in laboratory analysis.

Conflicts of Interest: The authors declare no conflict of interest.

References

1. Ragauskas, A.J.; Beckham, G.T.; Bidy, M.J.; Chandra, R.; Chen, F.; Davis, M.F.; Davison, B.H.; Dixon, R.A.; Gilna, P.; Keller, M.; et al. Lignin valorization: Improving lignin processing in the biorefinery. *Science* **2014**, *344*, 1246843. [[CrossRef](#)]
2. Azadi, P.; Inderwildi, O.R.; Farnood, R.; King, D.A. Liquid fuels, hydrogen and chemicals from lignin: A critical review. *Renew. Sustain. Energy Rev.* **2013**, *21*, 506–523. [[CrossRef](#)]
3. Schuler, J.; Hornung, U.; Kruse, A.; Dahmen, N.; Sauer, J. Hydrothermal Liquefaction of Lignin. *J. Biomater. Nanobiotechnol.* **2017**, *8*, 96–108. [[CrossRef](#)]
4. Alekhina, M.; Ershova, O.; Ebert, A.; Heikkinen, S.; Sixta, H. Softwood kraft lignin for value-added applications: Fractionation and structural characterization. *Ind. Crops Prod.* **2015**, *66*, 220–228. [[CrossRef](#)]
5. Sahoo, S.; Seydibeyoğlu, M.Ö.; Mohanty, A.K.; Misra, M. Characterization of industrial lignins for their utilization in future value added applications. *Biomass Bioenergy* **2011**, *35*, 4230–4237. [[CrossRef](#)]
6. Chudziak, C.; Alberts, G.; Bauen, A. *Ramp Up of Lignocellulosic Ethanol in Europe to 2030 Final Report*; E4tech: London, UK, 2017.
7. Biermann, C.J. Pulping Fundamentals. In *Handbook of Pulping and Papermaking*; Biermann, C.J., Ed.; Elsevier: Amsterdam, The Netherlands, 1996; pp. 55–100. ISBN 9780120973620.
8. Xu, C.; Arancon, R.A.D.; Labidi, J.; Luque, R. Lignin depolymerisation strategies: Towards valuable chemicals and fuels. *Chem. Soc. Rev.* **2014**, *43*, 7485–7500. [[CrossRef](#)]
9. Solimene, R.; Cammarota, A.; Chirone, R.; Leoni, P.; Rossi, N.; Salatino, P. Devolatilization and Fragmentation of Solid Lignin-rich Residues from Bioethanol Production in Lab-scale Fluidized Bed Reactors. *Chem. Eng. Trans* **2016**, *50*, 79–84.
10. Akiya, N.; Savage, P.E. Roles of Water for Chemical Reactions in High-Temperature Water. *Chem. Rev.* **2002**, *102*, 2725–2750. [[CrossRef](#)]

11. Yuan, Z.; Cheng, S.; Leitch, M.; Xu, C.C. Hydrolytic degradation of alkaline lignin in hot-compressed water and ethanol. *Bioresour. Technol.* **2010**, *101*, 9308–9313. [[CrossRef](#)]
12. Nguyen, T.D.H.; Maschietti, M.; Åmand, L.E.; Vamling, L.; Olausson, L.; Andersson, S.I.; Theliander, H. The effect of temperature on the catalytic conversion of Kraft lignin using near-critical water. *Bioresour. Technol.* **2014**, *170*, 196–203. [[CrossRef](#)]
13. Jensen, M.M.; Djajadi, D.T.; Torri, C.; Rasmussen, H.B.; Madsen, R.B.; Venturini, E.; Vassura, I.; Becker, J.; Iversen, B.B.; Meyer, A.S.; et al. Hydrothermal Liquefaction of Enzymatic Hydrolysis Lignin: Biomass Pretreatment Severity Affects Lignin Valorization. *ACS Sustain. Chem. Eng.* **2018**, *6*, 5940–5949. [[CrossRef](#)]
14. Katahira, R.; Mittal, A.; McKinney, K.; Chen, X.; Tucker, M.P.; Johnson, D.K.; Beckham, G.T. Base-Catalyzed Depolymerization of Biorefinery Lignins. *ACS Sustain. Chem. Eng.* **2016**, *4*, 1474–1486. [[CrossRef](#)]
15. Nielsen, J.B.; Jensen, A.; Madsen, L.R.; Larsen, F.H.; Felby, C.; Jensen, A.D. Noncatalytic Direct Liquefaction of Biorefinery Lignin by Ethanol. *Energy Fuels* **2017**, *31*, 7223–7233. [[CrossRef](#)]
16. Belkheiri, T.; Mattsson, C.; Andersson, S.I.; Olausson, L.; Åmand, L.E.; Theliander, H.; Vamling, L. Effect of pH on Kraft Lignin Depolymerisation in Subcritical Water. *Energy Fuels* **2016**, *30*, 4916–4924. [[CrossRef](#)]
17. Xu, Y.; Isom, L.; Hanna, M.A. Adding value to carbon dioxide from ethanol fermentations. *Bioresour. Technol.* **2010**, *101*, 3311–3319. [[CrossRef](#)]
18. McAloon, A.; Taylor, F.; Yee, W.; Regional, E.; Ibsen, K.; Wooley, R.; Biotechnology, N. *Determining the Cost of Producing Ethanol from Corn Starch and Lignocellulosic Feedstocks*; NREL: Golden, CO, USA, 2000.
19. Restrepo-Valencia, S.; Walter, A. Techno-economic assessment of bio-energy with carbon capture and storage systems in a typical sugarcane mill in Brazil. *Energies* **2019**, *12*, 1129. [[CrossRef](#)]
20. Patel, R.N.; Bandyopadhyay, S.; Ganesh, A. Extraction of cardanol and phenol from bio-oils obtained through vacuum pyrolysis of biomass using supercritical fluid extraction. *Energy* **2011**, *36*, 1535–1542. [[CrossRef](#)]
21. Naik, S.N.; Goud, V.V.; Rout, P.K.; Dalai, A.K. Production of first and second generation biofuels: A comprehensive review. *Renew. Sustain. Energy Rev.* **2010**, *14*, 578–597. [[CrossRef](#)]
22. Montesantos, N.; Pedersen, T.H.; Nielsen, R.P.; Rosendahl, L.; Maschietti, M. Supercritical carbon dioxide fractionation of bio-crude produced by hydrothermal liquefaction of pinewood. *J. Supercrit. Fluids* **2019**, *149*, 97–109. [[CrossRef](#)]
23. Montesantos, N.; Pedersen, T.H.; Nielsen, R.P.; Rosendahl, L.A.; Maschietti, M. High-temperature extraction of lignocellulosic bio-crude by supercritical carbon dioxide. *Chem. Eng. Trans.* **2019**, *74*, 799–804.
24. Numan-Al-Mobin, A.M.; Kolla, P.; Dixon, D.; Smirnova, A. Effect of water–carbon dioxide ratio on the selectivity of phenolic compounds produced from alkali lignin in sub- and supercritical fluid mixtures. *Fuel* **2016**, *185*, 26–33. [[CrossRef](#)]
25. Heng, Y.; Quitain, A.T.; Yusup, S.; Uemura, Y.; Sasaki, M. Optimization of hydrothermal liquefaction of palm kernel shell and consideration of supercritical carbon dioxide mediation effect. *J. Supercrit. Fluids* **2018**, *133*, 640–646.
26. Miliotti, E.; Dell’Orco, S.; Lotti, G.; Rizzo, A.M.; Rosi, L.; Chiaramonti, D. Lignocellulosic Ethanol Biorefinery: Valorization of Lignin-Rich Stream through Hydrothermal Liquefaction. *Energies* **2019**, *12*, 723. [[CrossRef](#)]
27. Sluiter, A.; Hames, B.; Ruiz, R.; Scarlata, C.; Sluiter, J.; Templeton, D. *Determination of Sugars, Byproducts, and Degradation Products in Liquid Fraction Process Samples*; Technical Report NREL/TP-510-42623; NREL: Golden, CO, USA, 2008.
28. Miliotti, E.; Casini, D.; Lotti, G.; Pennazzi, S.; Rizzo, A.M.; Chiaramonti, D. Hydrothermal Carbonization of Digestate: Characterization of solid and liquid products. In Proceedings of the TC Biomass, Gas Technology Institute, Chicago, IL, USA, 27 June 2017.
29. Beckner, M.; Ivey, M.L.; Phister, T.G. Microbial contamination of fuel ethanol fermentations. *Let. Appl. Microbiol.* **2011**, *53*, 387–394. [[CrossRef](#)] [[PubMed](#)]
30. Nissen, T.L.; Hamann, C.W.; Kielland-Brandt, M.C.; Nielsen, J.; Villadsen, J. Anaerobic and aerobic batch cultivations of *Saccharomyces cerevisiae* mutants impaired in glycerol synthesis. *Yeast* **2000**, *16*, 463–474. [[CrossRef](#)]
31. Toor, S.S.; Rosendahl, L.; Rudolf, A. Hydrothermal liquefaction of biomass: A review of subcritical water technologies. *Energy* **2011**, *36*, 2328–2342. [[CrossRef](#)]
32. Peterson, A.A.; Vogel, F.; Lachance, R.P.; Fröling, M.; Antal, J., Jr.; Tester, J.W. Thermochemical biofuel production in hydrothermal media: A review of sub- and supercritical water technologies. *Energy Environ. Sci.* **2008**, *1*, 32–65. [[CrossRef](#)]

33. Wang, C.; Li, H.; Li, M.; Bian, J.; Sun, R. Revealing the structure and distribution changes of Eucalyptus lignin during the hydrothermal and alkaline pretreatments. *Sci. Rep.* **2017**, *7*, 1–10. [CrossRef]
34. Bobleter, O. Hydrothermal degradation of polymers derived from plants. *Prog. Polym. Sci.* **1994**, *19*, 797–841. [CrossRef]
35. Arturi, K.R.; Strandgaard, M.; Nielsen, R.P.; Søgaard, E.G.; Maschietti, M. Hydrothermal liquefaction of lignin in near-critical water in a new batch reactor: Influence of phenol and temperature. *J. Supercrit. Fluids* **2017**, *123*, 28–39. [CrossRef]
36. Sasaki Mitsuru, W.; Motonobu, G. Recovery of phenolic compounds through the decomposition of lignin in near and supercritical water. *Chem. Eng. Process. Process Intensif.* **2008**, *47*, 1609–1619.
37. Barbier, J.; Charon, N.; Dupassieux, N.; Loppinet-Serani, A.; Mahé, L.; Ponthus, J.; Courtiade, M.; Ducrozet, A.; Quoineaude, A.A.; Cansell, F. Hydrothermal conversion of lignin compounds. A detailed study of fragmentation and condensation reaction pathways. *Biomass Bioenergy* **2012**, *46*, 479–491. [CrossRef]
38. Lawson, J.J.R.; Klein, M.M.T. Influence of Water on Guaiacol Pyrolysis. *Ind. Eng. Chem. Fundam.* **1985**, *24*, 203–208. [CrossRef]
39. Miller, J.E.; Evans, L.R.; Mudd, J.E.; Brown, K.A. *Batch Microreactor Studies of Lignin Depolymerization by Bases. 2. Aqueous Solvents*; Sandia National Labs.: Albuquerque, NM, USA, 2002.
40. Porzio, G.F.; Prussi, M.; Chiamonti, D.; Pari, L. Modelling lignocellulosic bioethanol from poplar: Estimation of the level of process integration, yield and potential for co-products. *J. Clean. Prod.* **2012**, *34*, 66–75. [CrossRef]
41. Robak, K.; Balcerek, M. Review of second generation bioethanol production from residual biomass. *Food Technol. Biotechnol.* **2018**, *56*, 174–187. [CrossRef] [PubMed]
42. Möller, M.; Harnisch, F.; Schröder, U. Hydrothermal liquefaction of cellulose in subcritical water—the role of crystallinity on the cellulose reactivity. *Rsc Adv.* **2013**, *3*, 11035–11044. [CrossRef]
43. Pedersen, T.H. HydroThermal Liquefaction of Biomass and Model Compounds. Ph.D. Thesis, Aalborg Universitet, Aalborg Universitetsforlag, Aalborg, Denmark, 2015.
44. Pedersen, T.H.; Rosendahl, L.A. Production of fuel range oxygenates by supercritical hydrothermal liquefaction of lignocellulosic model systems. *Biomass Bioenergy* **2015**, *83*, 206–215. [CrossRef]
45. Aden, A.; Ruth, M.; Ibsen, K.; Jechura, J.; Neeves, K.; Sheehan, J.; Wallace, B.; Montague, L.; Slayton, A.; Lukas, J. *Lignocellulosic Biomass to Ethanol Process Design and Economics Utilizing Co-Current Dilute Acid Prehydrolysis and Enzymatic Hydrolysis for Corn Stover*; NREL: Golden, CO, USA, 2002.
46. Villadsen, S.R.; Dithmer, L.; Forsberg, R.; Becker, J.; Rudolf, A.; Iversen, S.B.; Glasius, M. Development and Application of Chemical Analysis Methods for Investigation of Bio-Oils and Aqueous Phase from Hydrothermal Liquefaction of Biomass. *Energy Fuels* **2012**, *26*, 6988–6998. [CrossRef]
47. Jensen, M.M.; Madsen, R.B.; Becker, J.; Iversen, B.B.; Glasius, M. Products of hydrothermal treatment of lignin and the importance of ortho-directed repolymerization reactions. *J. Anal. Appl. Pyrolysis* **2017**, *126*, 371–379. [CrossRef]
48. Biswas, B.; Singh, R.; Kumar, J.; Khan, A.A.; Krishna, B.B.; Bhaskar, T. Slow pyrolysis of prot, alkali and dealkaline lignins for production of chemicals. *Bioresour. Technol.* **2015**, *213*, 319–326. [CrossRef]
49. Li, S.; Lundquist, K. A new method for the analysis of phenolic groups in lignins by ¹H NMR spectrometry. *Nord. Pulp Pap. Res. J.* **1994**, *09*, 191–195. [CrossRef]
50. Chu, S.; Subrahmanyam, A.V.; Huber, G.W. The pyrolysis chemistry of a β -O-4 type oligomeric lignin model compound. *Green Chem.* **2013**, *15*, 125–136. [CrossRef]
51. Cheng, S.; Wilks, C.; Yuan, Z.; Leitch, M.; Xu, C. Hydrothermal degradation of alkali lignin to bio-phenolic compounds in sub/supercritical ethanol and water–ethanol co-solvent. *Polym. Degrad. Stab.* **2012**, *97*, 839–848. [CrossRef]
52. Ingram, L.; Mohan, D.; Bricka, M.; Steele, P.; Strobel, D.; Crocker, D.; Mitchell, B.; Mohammad, J.; Cantrell, K.; Pittman, C.U.J. Pyrolysis of Wood and Bark in an Auger Reactor: Physical Properties and Chemical Analysis of the Produced Bio-oils. *Energy Fuels* **2008**, *22*, 614–625. [CrossRef]
53. Ralph, S.; Ralph, J.; Landucci, L.L. NMR Database of Lignin and Cell Wall Model Compounds 2009. Available online: https://www.glbc.org/databases_and_software/nmrdatabase/NMR_DataBase_2009_Complete.pdf (accessed on 27 February 2020).
54. Mullen, C.A.; Strahan, G.D.; Boateng, A.A. Characterization of various fast-pyrolysis bio-oils by NMR spectroscopy. *Energy Fuels* **2009**, *23*, 2707–2718. [CrossRef]

55. Chern, S.; Tu, H.; Materials, A. The Thermochemical Conversion of Lactic Acid in Subcritical and Supercritical Water. *Eng. Technol. Int. J. Chem. Mol.* **2017**, *11*, 98–102.
56. Islam, M.N.; Taki, G.; Rana, M.; Park, J.H. Yield of Phenolic Monomers from Lignin Hydrothermolysis in Subcritical Water System. *Ind. Eng. Chem. Res.* **2018**, *57*, 4779–4784. [[CrossRef](#)]
57. Singh, R.; Prakash, A.; Dhiman, S.K.; Balagurumurthy, B.; Arora, A.K.; Puri, S.K.; Bhaskar, T. Hydrothermal conversion of lignin to substituted phenols and aromatic ethers. *Bioresour. Technol.* **2014**, *165*, 319–322. [[CrossRef](#)]
58. Pińkowska, H.; Wolak, P.; Złocińska, A. Hydrothermal decomposition of alkali lignin in sub- and supercritical water. *Chem. Eng. J.* **2012**, *187*, 410–414. [[CrossRef](#)]
59. Wahyudiono; Kanetake, T.; Sasaki, M.; Goto, M. Decomposition of a Lignin Model Compound under Hydrothermal Conditions. *Chem. Eng. Technol.* **2007**, *30*, 1113–1122. [[CrossRef](#)]
60. Jegers, H.E.; Klein, M.T. Primary and Secondary Lignin Pyrolysis Reaction Pathways. *Ind. Eng. Chem. Process Des. Dev.* **1985**, *24*, 173–183. [[CrossRef](#)]
61. Numan-Al-Mobin, A.M.; Voeller, K.; Bilek, H.; Kozliak, E.; Kubatova, A.; Raynie, D.; Dixon, D.; Smirnova, A. Selective Synthesis of Phenolic Compounds from Alkali Lignin in a Mixture of Sub- and Supercritical Fluids: Catalysis by CO₂. *Energy and Fuels* **2016**, *30*, 2137–2143. [[CrossRef](#)]
62. Tabasinejad, F.; Moore, R.G.; Mehta, S.A.; Van Fraassen, K.C.; Barzin, Y.; Rushing, J.A.; Newsham, K.E. Water solubility in supercritical methane, nitrogen, and carbon dioxide: Measurement and modeling from 422 to 483 K and pressures from 3.6 to 134 MPa. *Ind. Eng. Chem. Res.* **2011**, *50*, 4029–4041. [[CrossRef](#)]
63. Takenouchi, S.; Kennedy, G.C. The Binary System H₂O-CO₂ at High Temperature and Pressures. *Am. J. Sci.* **1964**, *262*, 1055–1074. [[CrossRef](#)]
64. Pipitone, G.; Zoppi, G.; Bocchini, S.; Rizzo, A.M.; Chiaramonti, D.; Pirone, R.; Bensaid, S. Aqueous phase reforming of the residual waters derived from lignin-rich hydrothermal liquefaction: Investigation of representative organic compounds and actual biorefinery streams. *Catal. Today* **2019**. [[CrossRef](#)]
65. Wilson, A.N.; Dutta, A.; Black, B.A.; Mukarakate, C.; Schaidle, J.A.; Michener, W.E.; Beckham, G.T.; Nimlos, M.R. Valorization of Aqueous Waste Streams from Thermochemical Biorefineries. *Green Chem.* **2019**, *21*, 4217–4230. [[CrossRef](#)]
66. Davidson, S.D.; Lopez-Ruiz, J.A.; Zhu, Y.; Cooper, A.R.; Albrecht, K.O.; Dagle, R.A. Strategies to Valorize Hydrothermal Liquefaction-Derived Aqueous Phase into Fuels and Chemicals. *ACS Sustainable Chem. Eng.* **2019**, *7*, 19889–19901. [[CrossRef](#)]
67. INCO. *Corrosion Resistance of the Austenitic Chromium-Nickel Stainless Steels in Chemical Environments*; INCO: New York, NY, USA, 1963.



© 2020 by the authors. Licensee MDPI, Basel, Switzerland. This article is an open access article distributed under the terms and conditions of the Creative Commons Attribution (CC BY) license (<http://creativecommons.org/licenses/by/4.0/>).